COMPRESSIVE OPTICAL DEFLECTOMETRIC TOMOGRAPHY

Adriana González

ICTEAM/UCL

March 26th, 2014

ISPGroup - ICTEAM - UCL

ISP Group

http://sites.uclouvain.be/ispgroup

Université catholique de Louvain, Louvain-la-Neuve, Belgium. ISP Group

- 4 Professors
- 17 researchers
- 12 PhD students

Compressed Sensing Group

Prof. Laurent Jacques

Prof. Christophe De Vleeschouwer

Dr. Prasad Sudhakar

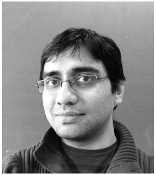

Kévin Degraux

Outline

1. Optical Deflectometric Tomography

2. Compressiveness in RIM Reconstruction

3. Compressiveness in Acquisition

Outline

1. Optical Deflectometric Tomography
2. Compressiveness in RIM Reconstruction
3. Compressiveness in Acquisition

Optical Deflectometric Tomography

Interest

- Optical characterization of (transparent) objects

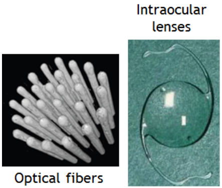

ODT

- Tomographic Imaging Modality
- Measures light deviation caused by the difference in the object refractive index

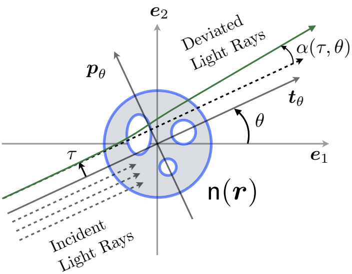

Schlieren Deflectometer

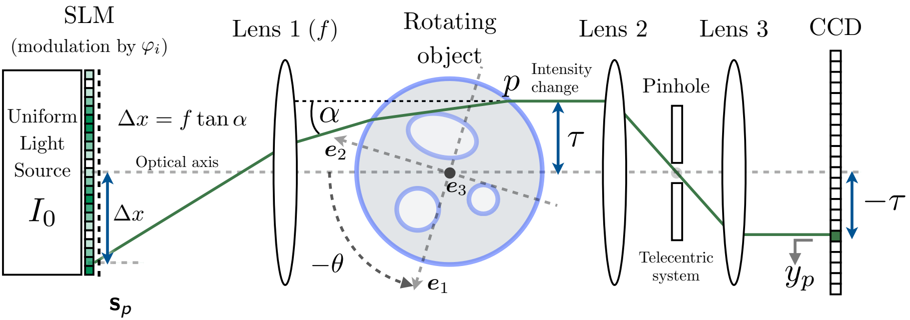

$$\mathbf{y}_p = \langle \mathbf{s}_p, \boldsymbol{\varphi}_i \rangle$$

Schlieren Deflectometer

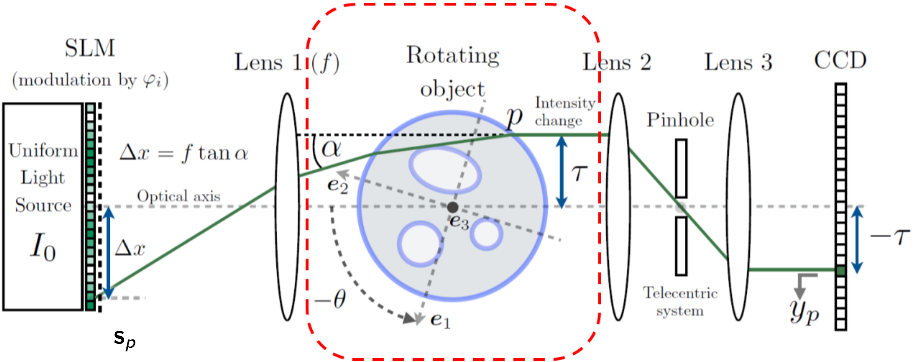

$$\mathbf{y}_p = \langle \mathbf{s}_p, \varphi_i \rangle$$

1 Compressiveness in RIM reconstruction

- φ sinusoidal pattern $\Rightarrow$ 4 shifted patterns φ_1, φ_2, φ_3, φ_4 $\Rightarrow$ 4 measurements to recover α
- Assuming deflections at one point
- Objects RIM variation only on $\mathbf{e}_1 - \mathbf{e}_2 \Rightarrow \alpha$, 2-D slices

Schlieren Deflectometer

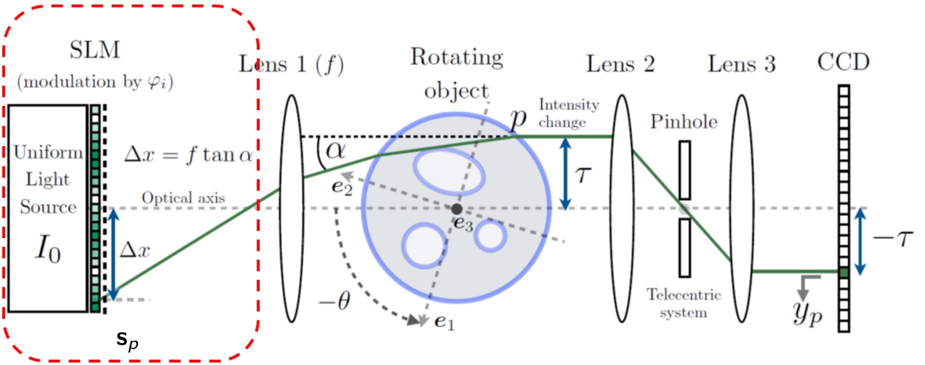

$$\mathbf{y}_p = \langle \mathbf{s}_p, \varphi_i \rangle$$

2 Compressiveness in acquisition

- Deflections produced by several points
- Objects RIM variation also on $\mathbf{e}_3 \Rightarrow \alpha$ and β, 3-D volume
- M binary modulation patterns φ_i to eliminate nonlinearities

Outline

1 Optical Deflectometric Tomography

2 Compressiveness in RIM Reconstruction

3 Compressiveness in Acquisition

Joint work with Prof. Laurent Jacques and Prof. Christophe De Vleeschouwer from UCL and Dr. Philippe Antoine from Lambda-X

Problem

- To reconstruct the refractive index map of transparent materials from light deflection measurements (α) under **few** orientations (θ)

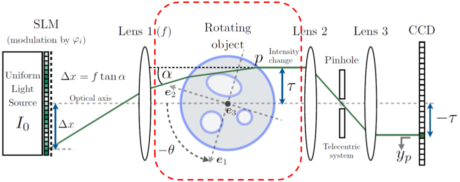

Assumption

- Objects are constant along the $\mathbf{e}_3$ direction
- Deflections at only one point

Intraocular lenses

Optical fibers

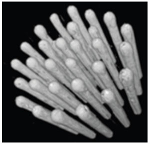

[1] A. González et al. iTWIST12
[2] P. Antoine et al. OPTIMESS 2012
[3] A. González et al. IPI Journal (2014)

Continuous facts

Mathematical Model

- Eikonal equation

  $\mathcal{R}$ curved : $\mathbf{r}(s) \to \frac{\mathrm{d}}{\mathrm{d}s}\big(\mathfrak{n}\frac{\mathrm{d}}{\mathrm{d}s}\mathbf{r}(s)\big) = \boldsymbol{\nabla}\mathfrak{n}$
- Approximation

  small $\alpha \to \mathcal{R}$ straight : $\mathbf{r}\cdot\mathbf{p}_\theta = \tau$

  error $< 10\%$

  $\Delta(\tau,\theta) = \sin(\alpha)$

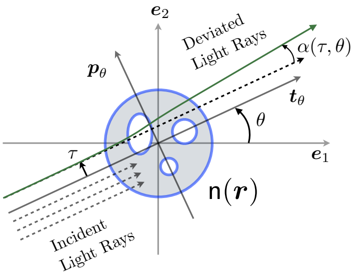

$$\Delta(\tau,\theta) = \frac{1}{\mathfrak{n}_\mathrm{r}}\int_{\mathbb{R}^2}\big(\boldsymbol{\nabla}\mathfrak{n}(\mathbf{r})\cdot\mathbf{p}_\theta\big)\;\delta(\tau - \mathbf{r}\cdot\mathbf{p}_\theta)\,\mathrm{d}^2\mathbf{r}$$

Deflectometric Central Slice Theorem

$$y(\omega,\theta) := \int_{\mathbb{R}}\Delta(\tau,\theta)\,e^{-2\pi i\tau\omega}\mathrm{d}\tau \;=\; \frac{2\pi i\omega}{\mathfrak{n}_\mathrm{r}}\,\widehat{\mathfrak{n}}(\omega\,\mathbf{p}_\theta)$$

$\widehat{\mathfrak{n}}(\omega\,\mathbf{p}_\theta)$: 2-D Fourier transform of $\widehat{\mathfrak{n}}$ in Polar grid

Discrete Forward Model

$$y = \frac{2\pi i(\delta r)^2}{\mathfrak{n}_r} \operatorname{diag}(\omega_{(1)}, \cdots, \omega_{(M)}) \, \widehat{\mathfrak{n}}$$

$$\Downarrow$$

$$\mathbf{y} = \mathbf{D}\mathbf{F}\boldsymbol{\mathfrak{n}} + \boldsymbol{\eta}$$

- $\mathfrak{n} \in \mathbb{R}^N$; Cartesian grid of $N = N_0^2$ pixels; sampling: δr
- $\mathbf{y} \in \mathbb{R}^M$; Polar grid of $M = N_\tau N_\theta$ pixels; sampling: $\delta\tau$, $\delta\theta$
- $\mathbf{D}$: $\frac{2\pi i(\delta r)^2}{\mathfrak{n}_r} \operatorname{diag}(\omega_{(1)}, \cdots, \omega_{(M)}) \in \mathbb{C}^{M \times M}$
- $\mathbf{F} \in \mathbb{C}^{M \times N}$: Non-equispaced Fourier Transform (NFFT) [4]
- $\boldsymbol{\eta} \in \mathbb{C}^M$: numerical computations, model discretization, model discrepancy, observation noise

[4] J. Keiner et al. (2009)

ODT vs. AT

$$\mathbf{y} = \mathbf{D}\mathbf{F}\mathfrak{n} + \boldsymbol{\eta}$$

- Main difference: Operator **D**
- Without noise $\boldsymbol{\eta} \rightarrow$ classical tomographic model

$$\tilde{\mathbf{y}} = \mathbf{D}^{-1}\mathbf{y} = \mathbf{F}\mathfrak{n}$$

- For $\boldsymbol{\eta} \neq 0 \rightarrow$ Not a classical tomographic model
  - $\boldsymbol{\eta}$: AWGN $\rightarrow \mathbf{D}^{-1}\boldsymbol{\eta}$ not homoscedastic

Observation: 1-D FT of sinograms along the τ direction

Absorption Tomography

Optical Deflection Tomography

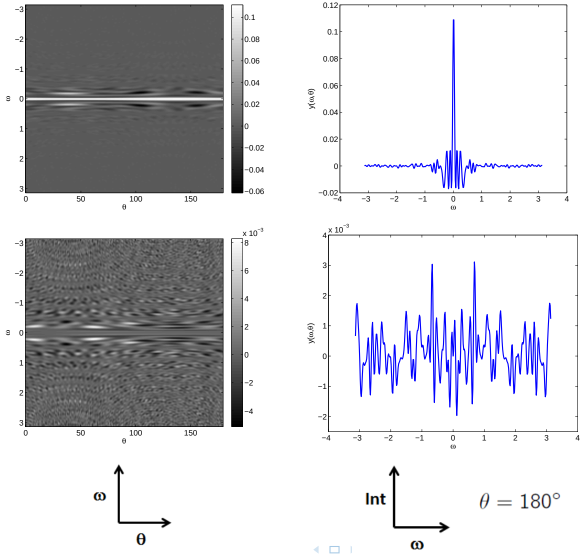

Naive Reconstruction Methods

$$\mathbf{y} = \mathbf{\Phi}\mathfrak{n} + \boldsymbol{\eta} = \mathbf{DF}\mathfrak{n} + \boldsymbol{\eta}$$

Filtered Back Projection

- Analytical method
- Solution $\tilde{\mathfrak{n}}_{\mathrm{FBP}}$:
  - Filtering the tomographic projections
    AT: ramp filter; ODT: Hilbert filter
  - Backprojecting in the spatial domain by angular integration

Minimum Energy Reconstruction

$$\tilde{\mathfrak{n}}_{\mathrm{ME}} = \mathbf{\Phi}^{\dagger}\mathbf{y} = \mathbf{\Phi}^{*}(\mathbf{\Phi}\mathbf{\Phi}^{*})^{-1}\mathbf{y} \quad \equiv \quad \tilde{\mathfrak{n}}_{\mathrm{ME}} = \arg\min_{\mathbf{u}\in\mathbb{R}^N} \|\mathbf{u}\|_2 \text{ s.t. } \mathbf{y} = \mathbf{\Phi}\mathbf{u}$$

Problems:

- Noise
- Compressiveness $\Rightarrow M(N_\theta) < N$
  $\Rightarrow$ ill-posed problem

Solution:
Regularization

Sparsity prior

Heterogeneous transparent materials with slowly varying refractive index separated by sharp interfaces

Intraocular lenses

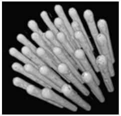

Optical fibers

TV and BV promote the perfect "cartoon shape" model

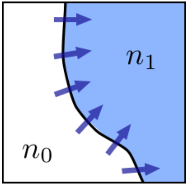

"Sparse" gradient

$\Downarrow$

Small Total Variation norm

$$\|\mathfrak{n}\|_{\mathsf{TV}} := \|\nabla\mathfrak{n}\|_{2,1}$$

Other priors

- Positive RIM

  $\Rightarrow \mathfrak{n} \succeq 0$

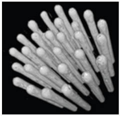

Optical fibers

Intraocular lenses

- The object is completely contained in the image. Pixels in the border are set to zero in order to guarantee uniqueness of the solution.

  $\Rightarrow \mathfrak{n}|_{\delta\Omega} = 0$

SOLUTION UNIQUENESS

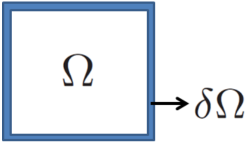

TV-ℓ_2 reconstruction and Noise

$$\mathbf{y} = \boldsymbol{\Phi}\mathfrak{n} + \boldsymbol{\eta} = \mathbf{DF}\mathfrak{n} + \boldsymbol{\eta}$$

TV-ℓ_2 Reconstruction

$$\tilde{\mathfrak{n}}_{\mathrm{TV}-\ell_2} = \arg\min_{\mathbf{u}\in\mathbb{R}^N} \|\mathbf{u}\|_{\mathsf{TV}} \ \text{ s.t. } \ \|\mathbf{y} - \boldsymbol{\Phi}\mathbf{u}\|_2 \leq \varepsilon, \ \mathbf{u} \succeq 0, \ \mathbf{u}_{\partial\Omega} = 0$$

Noise

- Observation noise $\rightarrow \sigma^2_{\mathsf{obs}}$
- Modeling error $\rightarrow$ ray tracing with Snell law $\approx 10\%$
- Interpolation noise $\rightarrow$ NFFT error (very small)

TV-ℓ_2 reconstruction

$$\mathbf{y} = \mathbf{\Phi}\mathfrak{n} + \boldsymbol{\eta} = \mathbf{DF}\mathfrak{n} + \boldsymbol{\eta}$$

TV-ℓ_2 Reconstruction

$$\tilde{\mathfrak{n}}_{\mathrm{TV}-\ell_2} = \arg\min_{\mathbf{u}\in\mathbb{R}^N} \|\mathbf{u}\|_{\mathrm{TV}} \text{ s.t. } \|\mathbf{y} - \mathbf{\Phi}\mathbf{u}\|_2 \leq \varepsilon,\ \mathbf{u} \succeq 0,\ \mathbf{u}_{\partial\Omega} = 0$$

$$\tilde{\mathfrak{n}}_{\mathrm{TV}-\ell_2} = \arg\min_{\mathbf{u}\in\mathbb{R}^N} \|\mathbf{u}\|_{\mathrm{TV}} + \imath_{\mathcal{C}}(\mathbf{\Phi}\mathbf{u}) + \imath_{\mathcal{P}_0}(\mathbf{u})$$

- Indicator function: $\imath_{\mathcal{X}}(x) = 0$ if $x \in \mathcal{X}$; $+\infty$ otherwise
- $\imath_{\mathcal{C}}$ and $\imath_{\mathcal{P}_0}$ are the indicator functions into the following convex sets:
  - $\mathcal{C} = \{\mathbf{v} \in \mathbb{C}^M : \|\mathbf{y} - \mathbf{v}\| \leq \varepsilon\}$
  - $\mathcal{P}_0 = \{\mathbf{u} \in \mathbb{R}^N : u_i \geq 0 \text{ if } i \in \mathrm{int}\ \Omega;\ u_i = 0 \text{ if } i \in \partial\Omega\}$

- Sum of 3 proper, lower semicontinuous, convex functions
- Reconstruction using CP algorithm [5] expanded in a product space

[5] A. Chambolle and T. Pock. Journal of Mathematical Imaging and Vision. (2011)

Reconstruction Algorithm

Chambolle-Pock (CP)

$$\min_{\mathbf{x}\in\mathcal{X}} \; F(\mathbf{K}\mathbf{x}) + G(\mathbf{x})$$

F, G: proper, lsc, convex; $\tau\sigma\|\mathbf{K}\|^2 < 1$

$$\begin{cases} \mathbf{v}^{(k+1)} = \mathrm{prox}_{\sigma F^\star}\left(\mathbf{v}^{(k)} + \sigma\mathbf{K}\bar{\mathbf{x}}^{(k)}\right) \\ \mathbf{x}^{(k+1)} = \mathrm{prox}_{\tau G}\left(\mathbf{x}^{(k)} - \tau\mathbf{K}^*\mathbf{v}^{(k+1)}\right) \\ \bar{\mathbf{x}}^{(k+1)} = 2\mathbf{x}^{(k+1)} - \mathbf{x}^{(k)} \end{cases}$$

- Proximal mapping
  f : proper, lsc, convex $\quad\Rightarrow\quad$ $\mathrm{prox}_{\sigma f}\,\mathbf{z} = \arg\min_{\bar{\mathbf{z}}}\; \sigma f(\bar{\mathbf{z}}) + \frac{1}{2}\|\bar{\mathbf{z}} - \mathbf{z}\|_2^2$
  e.g., $\mathrm{prox}_{\sigma\ell_1}\,\mathbf{z} = \mathrm{SoftTh}(\mathbf{z}, \sigma)$
- Conjugate function $F^\star(\mathbf{v}) = \max_{\bar{\mathbf{v}}}\; \langle \mathbf{v}, \bar{\mathbf{v}}\rangle - F(\bar{\mathbf{v}})$

CP Product-Space Expansion

$$\min_{\mathbf{x}\in\mathcal{X}} \sum_{j=1}^{t} F_j(\mathbf{K}_j\mathbf{x}) + G(\mathbf{x})$$

$$\mathbf{K} = \mathrm{diag}(\mathbf{K}_1, \cdots, \mathbf{K}_t)$$

$$\begin{cases} \mathbf{v}_j^{(k+1)} = \mathrm{prox}_{\sigma F_j^\star}\left(\mathbf{v}_j^{(k)} + \sigma\mathbf{K}_j\bar{\mathbf{x}}^{(k)}\right), \; j \in \{1, \cdots t\} \\ \mathbf{x}^{(k+1)} = \mathrm{prox}_{\frac{\tau}{t}H}\left(\mathbf{x}^{(k)} - \frac{\tau}{t}\sum_{j=1}^{t} \mathbf{K}_i^*\mathbf{v}_j^{(k+1)}\right) \\ \bar{\mathbf{x}}^{(k+1)} = 2\,\mathbf{x}^{(k+1)} - \mathbf{x}^{(k)} \end{cases}$$

Results: $\mathrm{TV}-\ell_2$ vs. ME & FBP

- Compressiveness and noise robustness

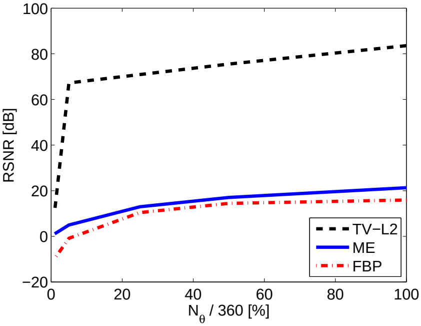

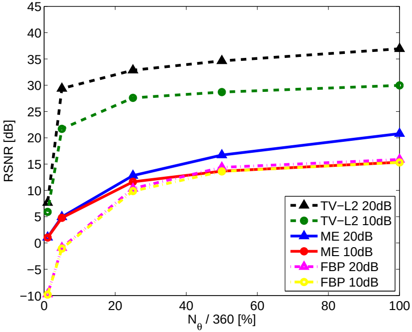

$$\mathrm{MSNR} = 20\log_{10}\frac{\|\boldsymbol{\Delta}\|_2}{\|\boldsymbol{\eta}\|_2} \qquad \mathrm{RSNR} = 20\log_{10}\frac{\|\mathfrak{n}\|_2}{\|\mathfrak{n}-\tilde{\mathfrak{n}}\|_2}$$

Results: TV-ℓ_2 vs. ME

- No measurement noise (MSNR $= \infty$)
- $N_\theta/360 = 25\%$

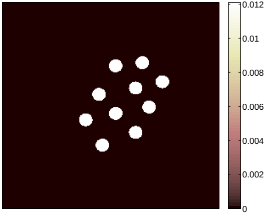

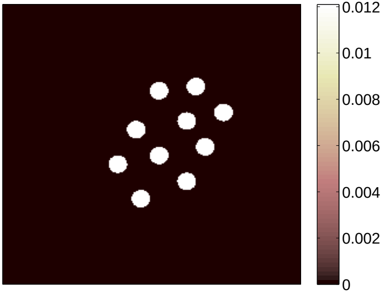

$\tilde{\mathbf{n}}_{\mathrm{TV}-\ell_2}$: RSNR = 71dB

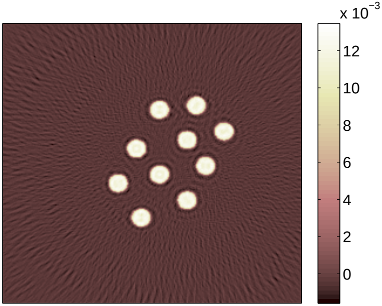

$\tilde{\mathbf{n}}_{\mathrm{ME}}$: RSNR = 13dB

Results: TV-ℓ_2 vs. ME

- No measurement noise ($\mathrm{MSNR} = \infty$)
- $N_\theta / 360 = 5\%$

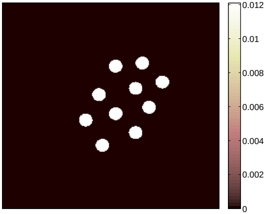

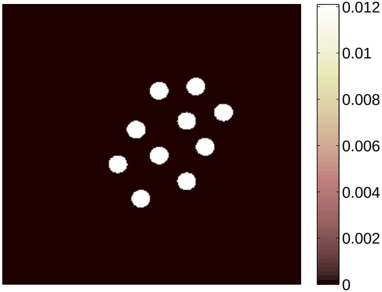

$\tilde{\mathfrak{n}}_{\mathrm{TV}-\ell_2}$: RSNR = 67dB

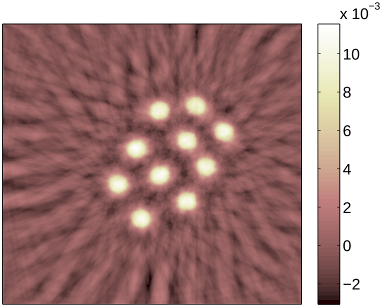

$\tilde{\mathfrak{n}}_{\mathrm{ME}}$: RSNR = 5dB

Results: TV-ℓ_2 vs. ME

- MSNR = 20dB
- $N_\theta / 360 = 25\%$

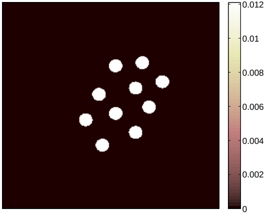

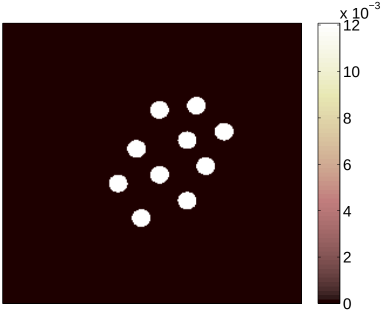

$\tilde{\mathbf{n}}_{\mathrm{TV}-\ell_2}$: RSNR = 39dB

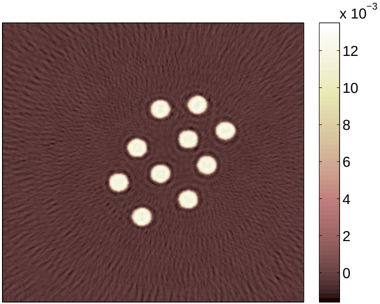

$\tilde{\mathbf{n}}_{\mathrm{ME}}$: RSNR = 13dB

Results: TV$-\ell_2$ Convergence

- Non-Adaptive: step-sizes constant along the iterations $\rightarrow \sigma = \tau = \frac{0.9}{\|\mathbf{K}\|}$
- Adaptive: step-sizes σ and τ are updated according to the residuals of the algorithm [6]

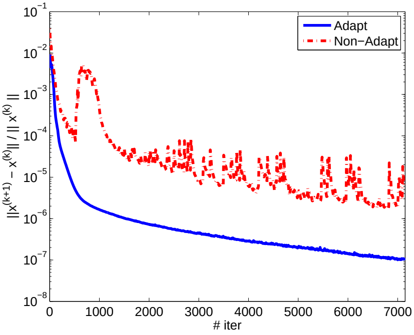

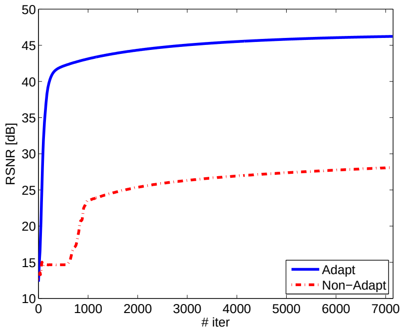

[6] T. Goldstein et al. Preprint (2013)

Experimental Results

- Bundle of 10 fibers immersed in an optical fluid
- MSNR $\approx$ 10dB
- $N_\theta = 60 \Rightarrow N_\theta/360 = 17\%$

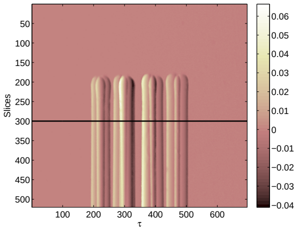

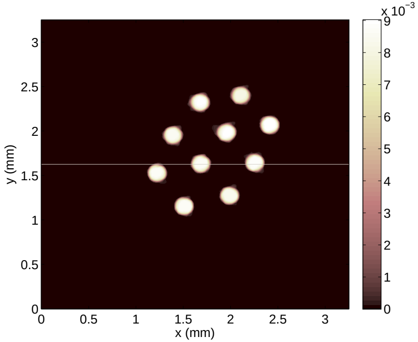

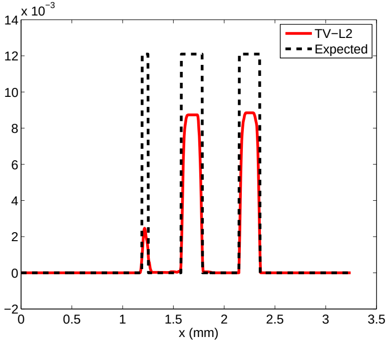

Outline

1 Optical Deflectometric Tomography

2 Compressiveness in RIM Reconstruction

3 Compressiveness in Acquisition

Schlieren Deflectometer

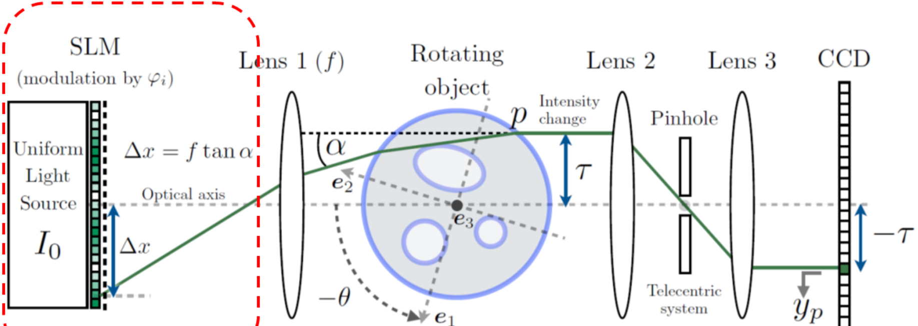

$\mathbf{s}_p$

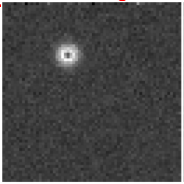

$$\mathbf{y}_p = \langle \mathbf{s}_p, \varphi_i \rangle$$

Framework

Work by Dr. Prasad Sudhakar and Prof. Laurent Jacques from UCL;
Xavier Dubois, Dr. Luc Joannes and Dr. Philippe Antoine from Lambda-X

Problem

- Objects RIM variation on $\mathbf{e}_1$, $\mathbf{e}_2$, $\mathbf{e}_3$ $\Rightarrow$ Local curvature at every p is characterized by the deflection spectra $\mathbf{s}_p(\tan\alpha, \beta) = \tilde{\mathbf{s}}_p(\alpha, \beta)$

Deflection Spectra

- Only measured indirectly
- **Sparse** : smooth objects $\Rightarrow$ controlled distortions

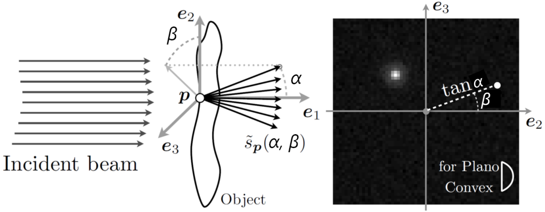

Objective

- To reconstruct the deflection map at all p using relatively few measurements (M) per orientation (θ)

[7] P. Sudhakar et al. IEEE ICASSP 2013
[8] P. Sudhakar et al. SampTA 2013

Forward model

- Location p in object $\Rightarrow$ $\mathbf{s}_p \in \mathbb{R}^{I \times I} = \mathbb{R}^L$ $\Rightarrow$ pixel p in CCD camera

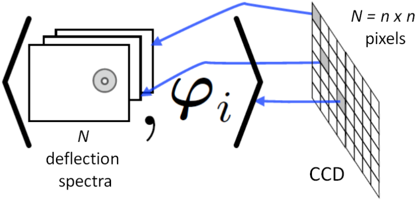

$$y_{i,p} = \langle \mathbf{s}_p, \varphi_i \rangle$$

- M Modulation patterns $\varphi_i \in \mathbb{R}^{I \times I} = \mathbb{R}^L$ $\Rightarrow$ $\mathbf{\Phi} = [\varphi_1^T \; \cdots \; \varphi_M^T]^T \in \mathbb{R}^{M \times L}$

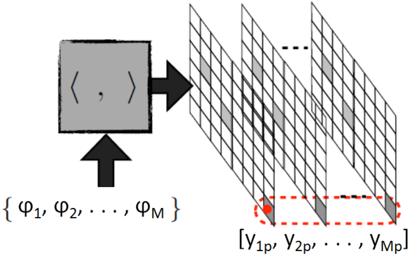

$$\mathbf{y}_p = \mathbf{\Phi} \mathbf{s}_p + \mathbf{n}$$

Challenges :

- Find a sparse $\mathbf{s}_p$ such that $\|\mathbf{y}_p - \mathbf{\Phi} \mathbf{s}_p\|_2 \leq \varepsilon$; $\|\mathbf{n}\|_2 \leq \varepsilon$
- Design of $\mathbf{\Phi}$ for $M < L$

Sparsity

- k-sparse signals and sparsity basis

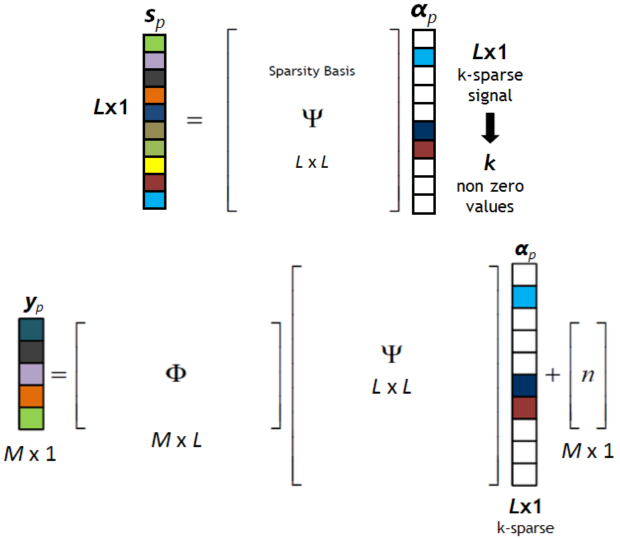

Sparse Recovery

- Sensing Basis

$$\mathbf{\Phi} = \mathbf{\Gamma}_\Omega^T$$

$\mathbf{\Gamma} \in \mathbb{R}^{L \times L}$: sensing basis

$\mathbf{\Gamma}_\Omega \in \mathbb{R}^{L \times M}$: random (uniform) selection of M columns of $\mathbf{\Gamma}$

$\Gamma_\Omega =$ 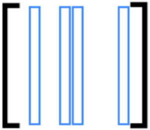

$\Omega \subset [L] := \{1, \cdots, L\}$

- **Objective** : Find a sparse $\mathbf{s}_p$ such that $\|\mathbf{y}_p - \mathbf{\Phi}\mathbf{s}_p\|_2 \leq \varepsilon$
- Basis Pursuit Denoising (**P1**)

$$\widehat{\boldsymbol{\alpha}_p} = \underset{\boldsymbol{\alpha}_p \in \mathbb{R}^L}{\arg\min} \|\boldsymbol{\alpha}_p\|_1 \text{ s.t. } \|\mathbf{y}_p - \mathbf{\Phi}\mathbf{\Psi}\boldsymbol{\alpha}_p\|_2 \leq \varepsilon \qquad \widehat{\mathbf{s}_p} = \mathbf{\Psi}\widehat{\boldsymbol{\alpha}_p}$$

- (**P1**) succeeds if $M = \mathcal{O}\left(\mu^2 k \log^4(L)\right)$

$$\mu = \sqrt{L} \max_{1 \leq i,j \leq L} |\langle \Gamma_j, \psi_i \rangle| \Rightarrow \text{Coherence between } \mathbf{\Gamma} \text{ and } \mathbf{\Psi}$$

  - $1 \leq \mu \leq \sqrt{L}$: $\downarrow \mu$ ($\mathbf{\Gamma}$ and $\mathbf{\Psi}$ less coherent) $\Rightarrow \downarrow M$
  - e.g. Fourier-Dirac are maximally incoherent $\Rightarrow \mu = 1$

Sensing Basis

- Compressiveness ($M < L$) $\rightarrow$ Sensing basis $\mathbf{\Gamma}$ incoherent with sparsity basis $\mathbf{\Psi}$
  Spread Spectrum Compressive Sensing [9]: random phase modulation of $\mathbf{s}_p$ to make sensing and sparsity bases incoherent
  - Spread Spectrum matrix: $\mathbf{M} = \mathrm{diag}(\mathbf{m}) \in \mathbb{R}^{L \times L}$, $|m_i| = 1$ (e.g. Rademacher)

$$\mathbf{\Phi} = \mathbf{\Gamma}_\Omega^T \mathbf{M} \quad \Rightarrow \quad \mathbf{y}_p = \mathbf{\Gamma}_\Omega^T \mathbf{M} \mathbf{\Psi} \alpha_p + \mathbf{n}$$

  - For universal sensing bases ($|\mathbf{\Gamma}_{ij}| =$ const., e.g., Fourier, Hadamard)
    $\rightarrow$ Successful recovery if $M \geq C_\rho k \log^5(L)$ with probability $1 - \mathcal{O}(N^{-\rho})$
- Sensing matrix $\mathbf{\Gamma}$ needs to satisfy 3 criteria:
  - Randomness for optimal measurements
  - Binary sensing matrix entries to avoid non-linearities
  - Structured measurements for fast computations

$$\mathbf{\Gamma} = \mathbf{H} : \text{ Hadamard basis} \qquad \mathbf{H}^T \mathbf{M} \in \{\pm 1\}^{L \times L}$$

- Physical constraints $\rightarrow$ non-negative, real-valued sensing matrix entries

$$\mathbf{\Phi} = \frac{1}{2} \left(\mathbf{H}_\Omega^T \mathbf{M} + \mathbf{1}_L \mathbf{1}_L^T \right) \in \{0, 1\}^{M \times L}$$

[9] G. Puy et al. Journal on Adv. in Sig. Proc. (2012)

Deflection spectrum reconstruction

$$\mathbf{y} = \mathbf{\Phi}\mathbf{s}_p + \mathbf{n} = \frac{1}{2}\left(\mathbf{H}_\Omega^T\mathbf{M} + \mathbf{1}_L\mathbf{1}_L^T\right)\mathbf{\Psi}\boldsymbol{\alpha}_p + \mathbf{n}$$

$\mathbf{\Psi}$: Daubechies 9 wavelet basis

$$\widehat{\boldsymbol{\alpha}_p} = \underset{\boldsymbol{\alpha}_p \in \mathbb{R}^L}{\arg\min} \|\boldsymbol{\alpha}_p\|_1 \text{ s.t. } \|\mathbf{y}_p - \mathbf{\Phi}\mathbf{\Psi}\boldsymbol{\alpha}_p\|_2 \leq \varepsilon; \ \mathbf{\Psi}\boldsymbol{\alpha}_p \succeq 0 \qquad \hat{\mathbf{s}}_p = \mathbf{\Psi}\widehat{\boldsymbol{\alpha}_p}$$

$$\widehat{\boldsymbol{\alpha}_p} = \underset{\boldsymbol{\alpha}_p \in \mathbb{R}^L}{\arg\min} \|\boldsymbol{\alpha}_p\|_1 + \imath_{\mathcal{C}}(\mathbf{\Phi}\mathbf{\Psi}\boldsymbol{\alpha}_p) + \imath_{\mathcal{P}}(\mathbf{\Psi}\boldsymbol{\alpha}_p) \qquad \hat{\mathbf{s}}_p = \mathbf{\Psi}\widehat{\boldsymbol{\alpha}_p}$$

- Indicator function: $\imath_{\mathcal{X}}(x) = 0$ if $x \in \mathcal{X}$; $+\infty$ otherwise
- $\imath_{\mathcal{C}}$ and $\imath_{\mathcal{P}}$ are the indicator functions into the following convex sets:
  - $\mathcal{C} = \{\mathbf{v} \in \mathbb{R}^M : \|\mathbf{y}_p - \mathbf{v}\| \leq \varepsilon\}$
  - $\mathcal{P} = \{\mathbf{u} \in \mathbb{R}^L : \mathbf{u}_+\}$

- Sum of 3 proper, lower semicontinuous, convex functions
- Reconstruction using CP algorithm expanded in a product space (non-adaptive)

Results

- Lambda-X NIMO system (SLM 64 × 64)
- Compressiveness

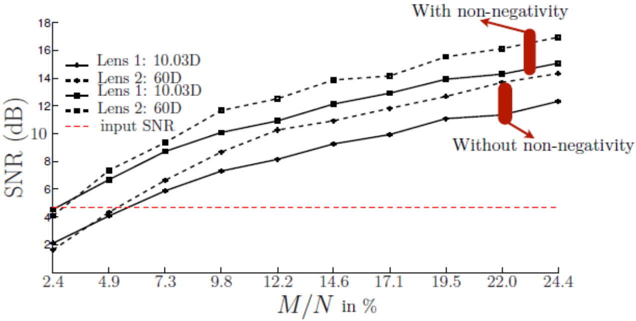

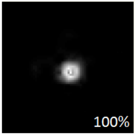

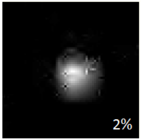

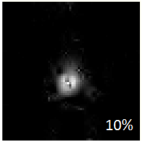

- Knowing the center of the spectral figure we can:
  - Recover deflections β and $\alpha = \text{atan}(\frac{r}{f_1})$ for each θ
    $\rightarrow$ RIM reconstruction

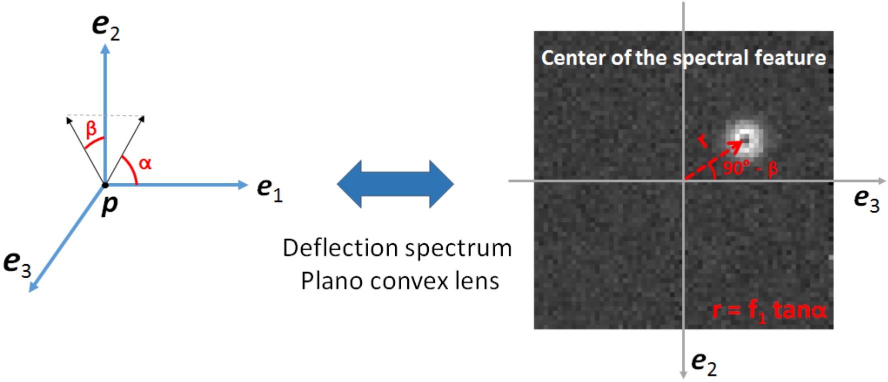

Information from Deflection Spectra

- Knowing the center of the spectral figure we can:
  - Describe an object surface

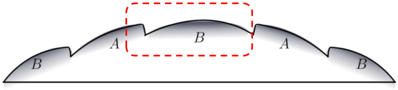

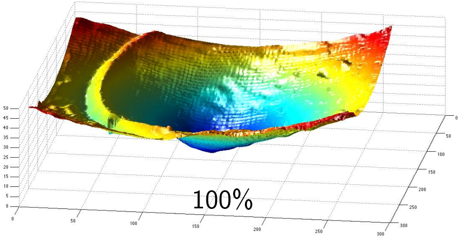

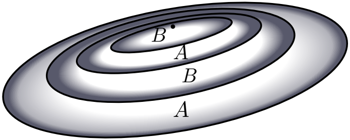

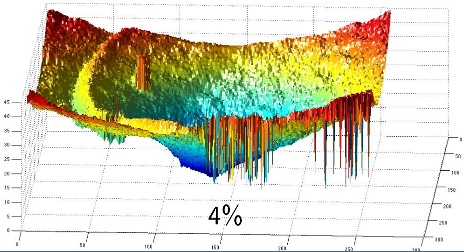

References

1 A. González et al. iTWIST12

2 P. Antoine et al. Proceedings of OPTIMESS 2012

3 A. González et al. To appear in IPI Journal (2014)

4 J. Keiner et al. ACM TOMS (2009)

5 A. Chambolle et al. Journal of Mathematical Imaging and Vision (2011)

6 T. Goldstein et al. Preprint, arXiv:1305.0546v1 (2013)

7 P. Sudhakar et al. IEEE ICASSP 2013

8 P. Sudhakar et al. SampTA 2013

9 G. Puy et al. Journal on Adv. in Sig. Proc. (2012)

Thank you!